# Supplementary Information

## Parallel measurement of dynamic changes in translation rates in single-cells

**Kyuho Han[1], Ariel Jaimovich[1,2], Gautam Dey[1], Davide Ruggero[3], Oded Meyuhas[4], Nahum Sonenberg[5], & Tobias Meyer[1]**

[1] Department of Chemical and Systems Biology, Stanford University

Stanford, CA 94305, USA

[2] Department of Biochemistry, Stanford University

Stanford, CA 94305, USA

[3] Helen Diller Family Comprehensive Cancer Center, University of California, San Francisco

San Francisco, CA 94143, USA

[4] Department of Biochemistry and Molecular Biology, The Institute for Medical Research Israel-Canada, Hebrew University-Hadassah Medical School

Jerusalem 91120, Israel

[5] Department of Biochemistry & Goodman Cancer Research Centre, McGill University

Montreal, Quebec H3A 1A3, Canada

Correspondence should be addressed to K.H. (kyuhohan@stanford.edu) or T.M.

(tobias1@stanford.edu)

Nature Methods: doi:10.1038/nmeth.2729

# Supplementary Fig. 1

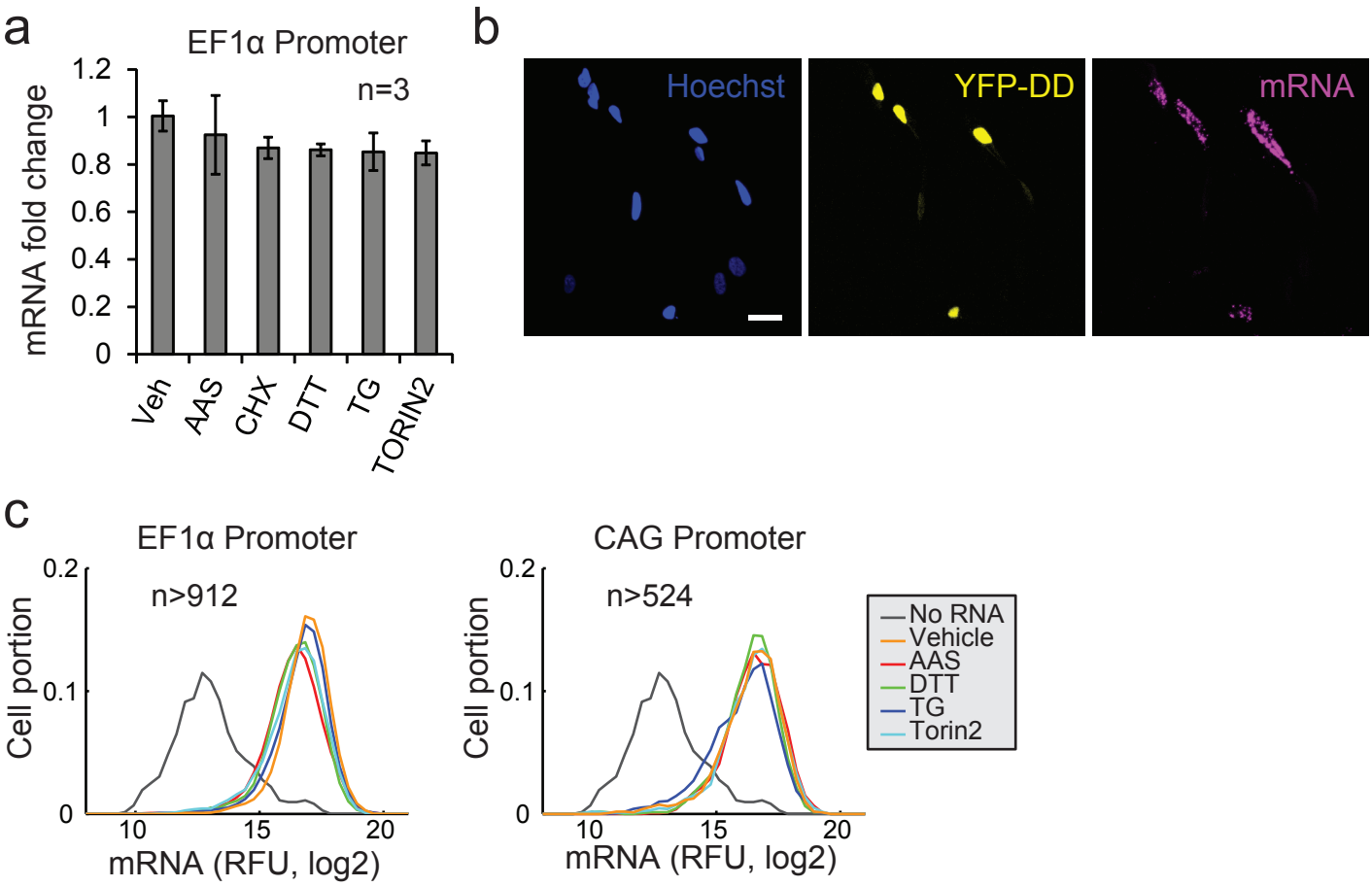


**Supplementary Figure 1: mRNA levels do not change significantly after the addition of various translational inhibitors**

**(a)** mRNA levels measured by quantitative RT-PCR 2 hours after the addition of the inhibitors. Data from three biological replicates. Error bar indicates s.e.m (n=3). **(b)** Control RNA FISH experiment using the probes targeting the ecDHFR sequence show that the probes only stained cells expressing the YFP-DD reporter. The RNA FISH staining is imaged in the Texas Red channel. **(c)** Histogram showing the single-cell mRNA distributions from the EF1A promoter (left panel) and the CAG promoter (right panel) 2 hours after the addition of the inhibitors. Cells without the reporter are used as a negative control.

# Supplementary Fig. 2

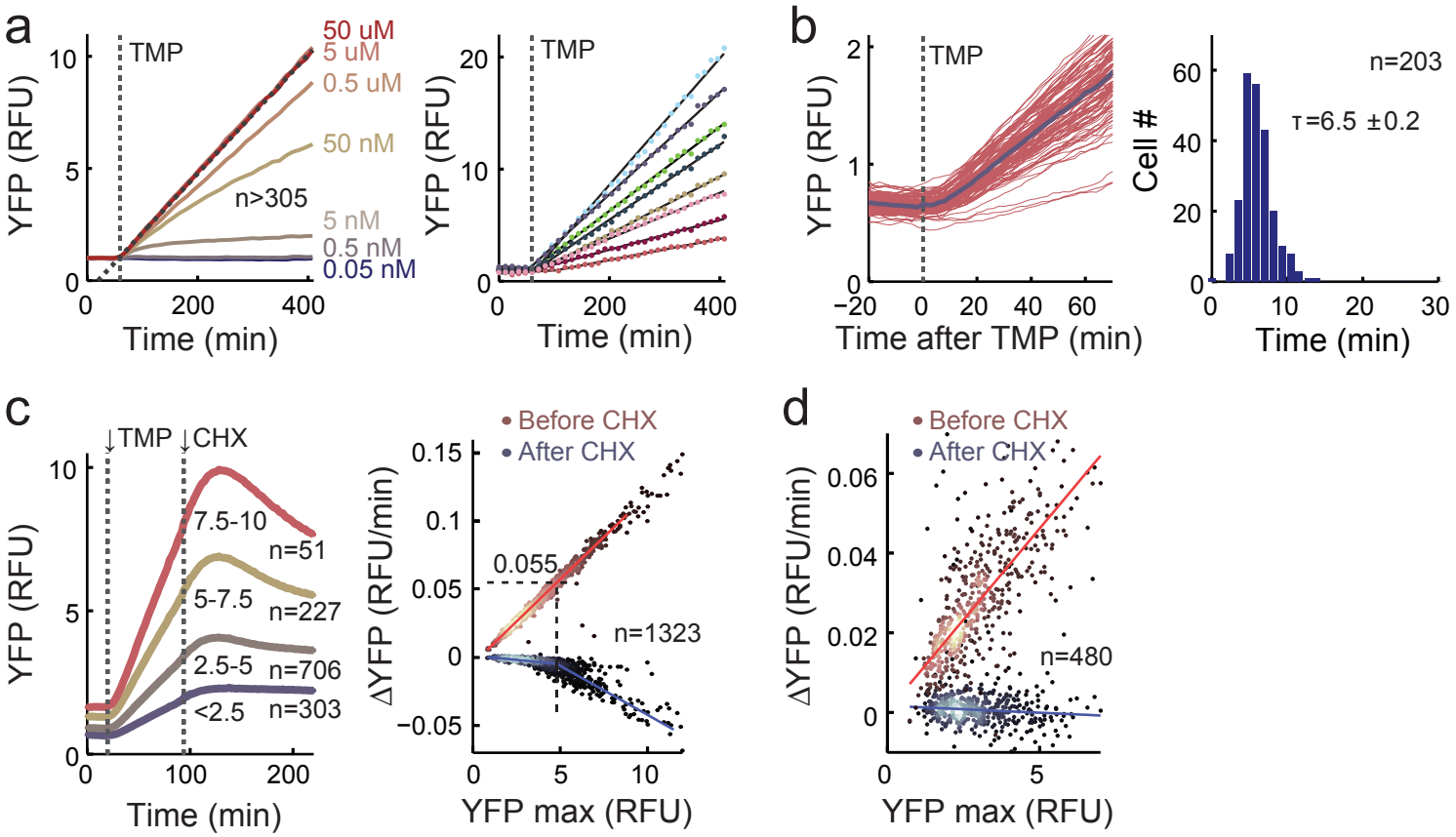


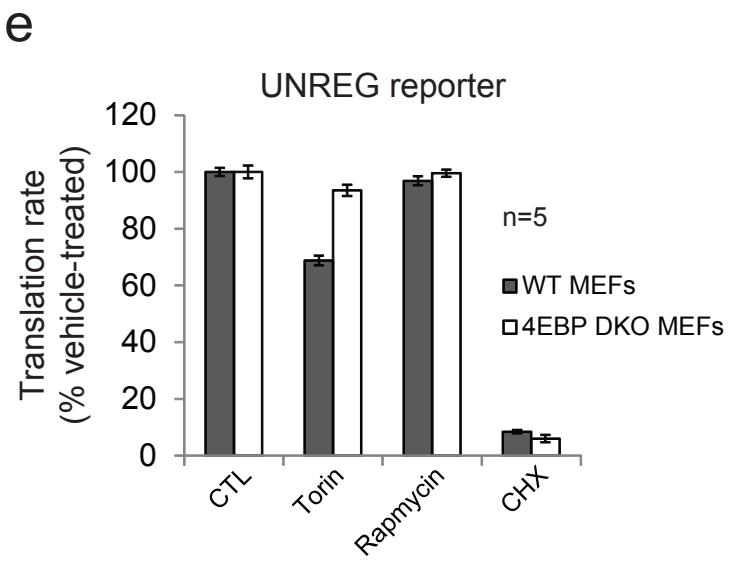


Nature Methods: doi:10.1038/nmeth.2729

**Supplementary Figure 2: Characterization of the YFP-DD reporter.**

**(a)** YFP accumulation curves in response to addition of varying amounts of TMP. The left panel shows the population averages of YFP values over time. The slopes of the curves saturate above 5 uM TMP. The right panel shows the YFP curves from several representative cells at 5 uM TMP. **(b)** Fast induction of YFP signals. After TMP addition, YFP signals start increasing almost immediately (left panel). Mean±s.e.m. for induction time is displayed using a histogram (right panel). **(c)** Degradation of the reporter after cycloheximide (CHX) addition. Cells are binned by their YFP levels at the time of CHX treatment, and the averages of YFP values from each bin are plotted over time to make the curves (Left panel). The ranges of YFP intensities used to bin cells are displayed below the curves. The right graph shows the scatter plots between YFP levels at the time of CHX addition and ΔYFPs before or after CHX addition. Red dot, ΔYFP before CHX; Blue dot, ΔYFP after CHX. The blue scatter plots indicate that there is negligible protein degradation in the cells which have a YFP accumulation rate of less than 0.055 RFU/min before CHX addition. **(d)** The same scatter plots generated from sorted cells with moderate levels of YFP-reporter expression indicate that there is no degradation even after CHX addition. **(e)** Inhibition of protein synthesis by several translation inhibitors are measured on wild type MEFs and 4E-BP DKO MEFs. Cells are treated with the following concentration of inhibitors for 2 hours and RTAs (% vehicle-treated cell) are measured during the last hour of the treatments. (Torin2: 250 nM, Rapamycin: 250 nM, Cycloheximide: 10ug/ml) Error bars represent s.e.m. of five biological replicates.

# Supplementary Fig. 3

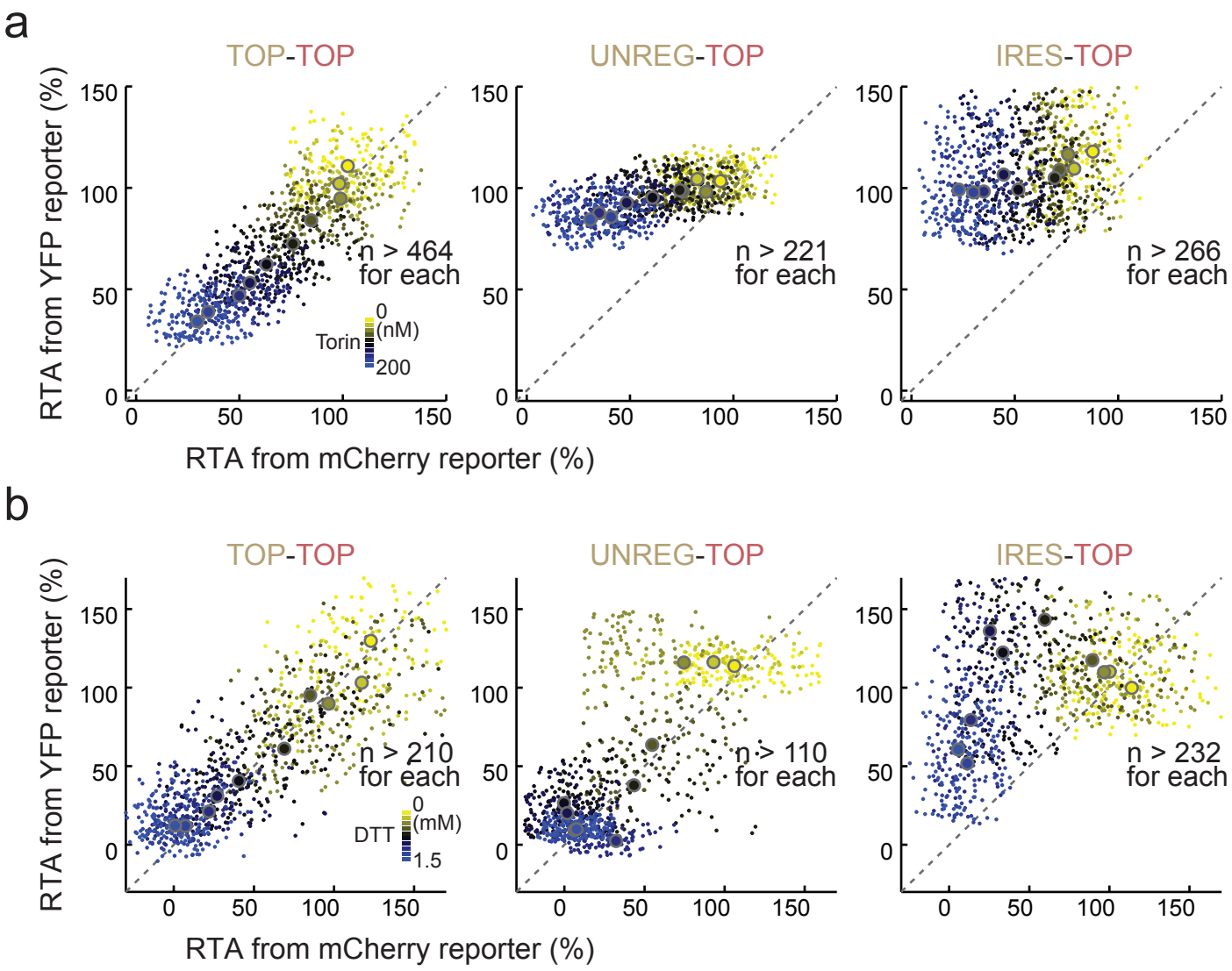


**Supplementary Figure 3: Single-cell scatter plots of the dual-color reporter**

**(a)** Scatter plots showing the RTA of different UTRs in response to the titration of Torin2 Each small dot marks the RTA of YFP (y-axis) and mCherry (x-axis) reporters from a single cell. Data from each Torin2 concentration are displayed in the same color. Torin2 concentrations are mapped onto the color bar, from top to bottom: 0 (nM), 6, 9, 13, 19, 30, 44, 67, 100, 200. Filled circles mark the population average for each concentration. Gray dotted line represents 1:1 diagonal. **(b)** Scatter plots showing the RTA of different UTRs in response to the titration of DTT levels. DTT concentrations mapped to the color bar: 0 (mM), 0.3, 0.45, 0.56, 0.66, 0.83, 1, 1.25, 1.5, 2.25.

Nature Methods: doi:10.1038/nmeth.2729

# Supplementary Fig. 4

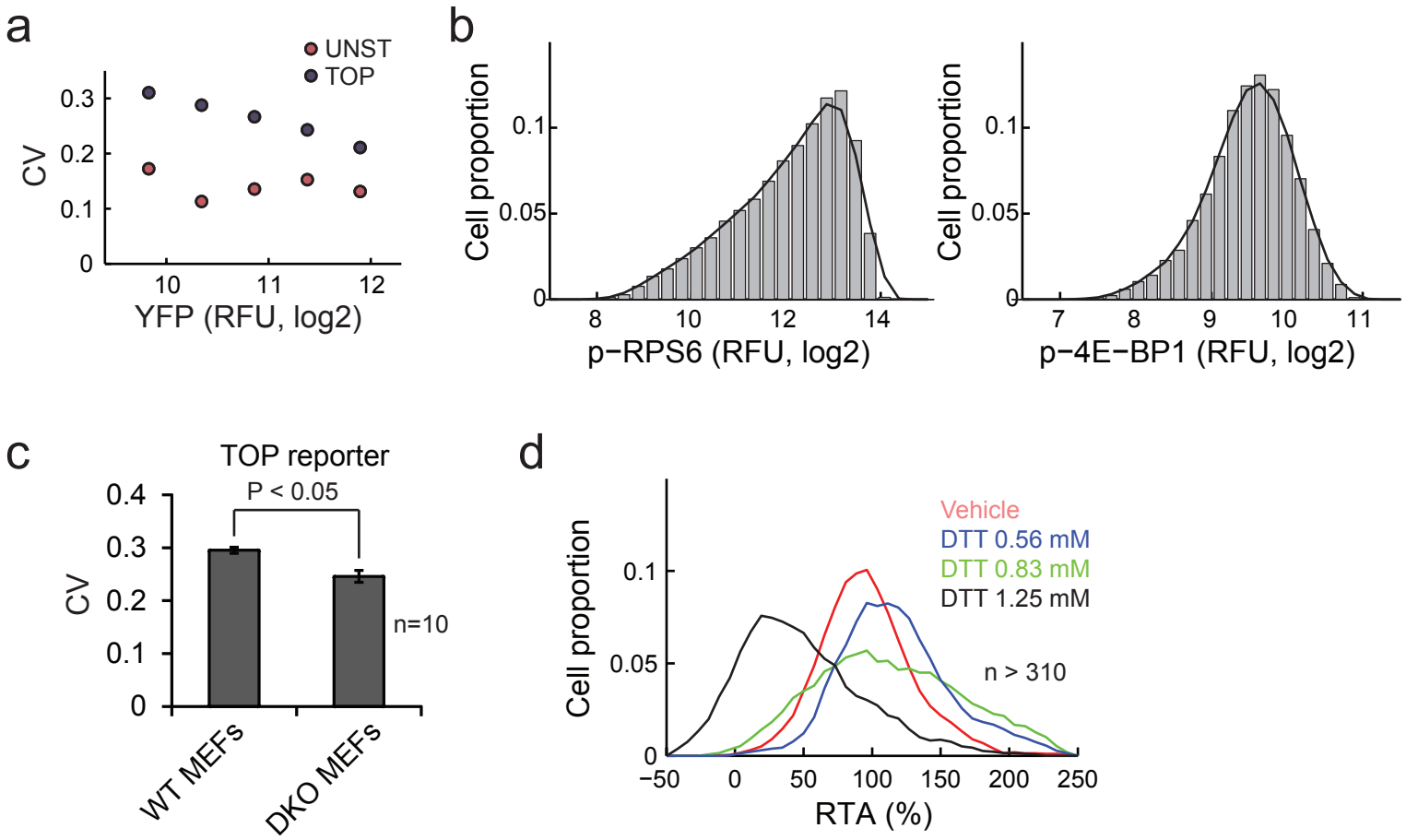


**Supplementary Figure 4: Analysis of temporal fluctuation in translation**

**(a)** Coefficient of variation (CV) of the TOP-reporter is higher than CV of the UNST-reporter across all levels of reporter expression. Cells are binned by their levels of reporter expression and CVs are calculated for each bin. **(b)** I.F. staining of phospho-RPS6 and phospho-4E-BPs shows higher heterogeneity in phosphorylation of RPS6 among single cells in the population. **(c)** Histogram of relative changes in IRES reporter activity in vehicle-treated cells and cells treated with different concentrations of DTT. **(c)** Bar graphs showing coefficient of variation (CV) of TOP reporters in wild type MEFs and 4E-BP DKO MEFs. Error bars indicate s.e.m. of 10 biological replicates. P=0.001 **(d)** Histogram of relative changes in IRES reporter activity in cells treated with different concentrations of DTT.

# Supplementary Fig. 5

a

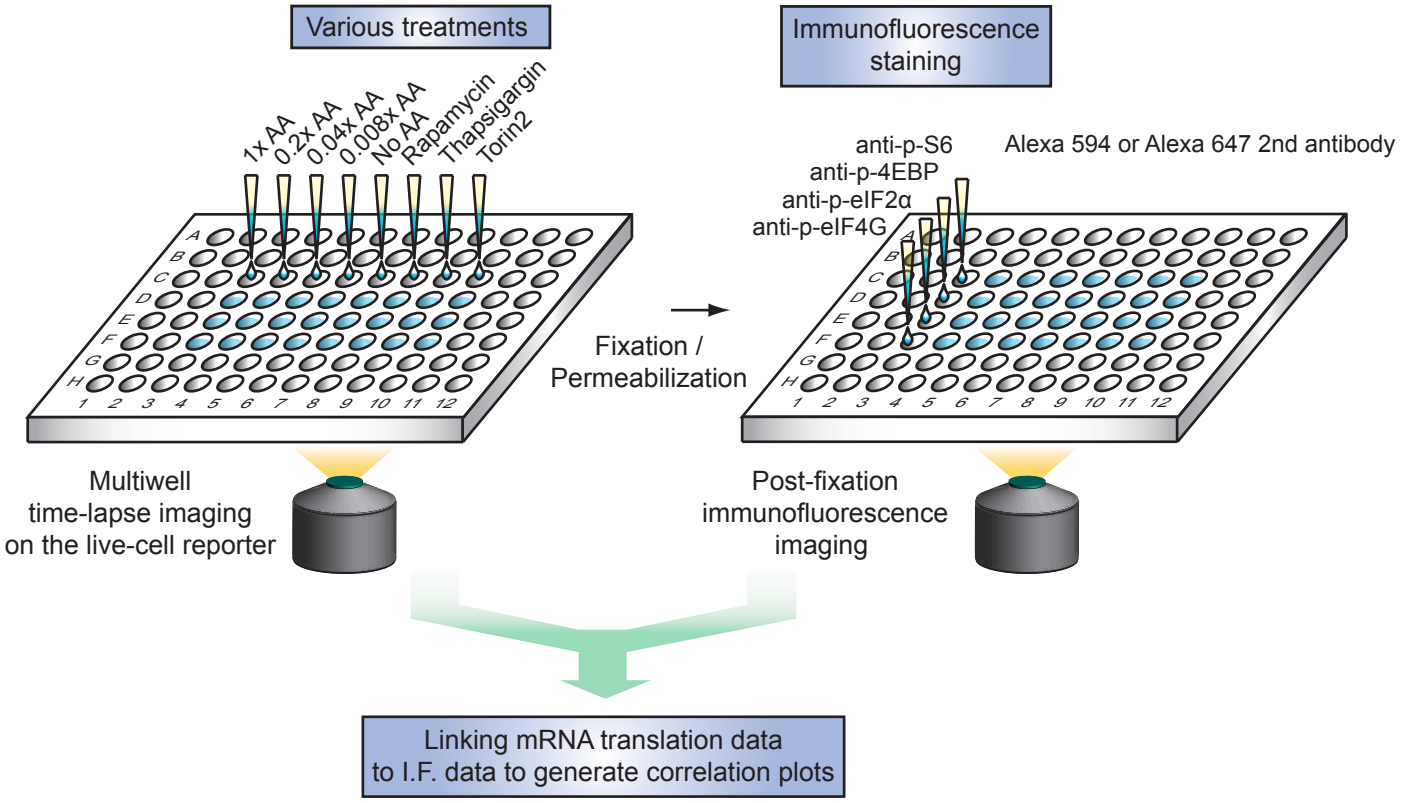


**Supplementary Figure 5: Schematic for post-live-cell imaging and generation of correlation plots between immunofluorescence staining and mRNA translation rates.**

**(a)** After time-lapse live-cell imaging, cells were fixed and immunostained with antibodies of interest. The x and y coordinates for re-imaging the immunostained cells are adjusted so that the current positions of cells are matched to the positions of the cells in the last frame of the live-cell imaging series. RTAs measured from the reporter during live-cell imaging and intensities of I.F. staining measured during fixed-cell imaging are linked to measure the correlation between the two measurements in each cell.

# Supplementary Fig. 6

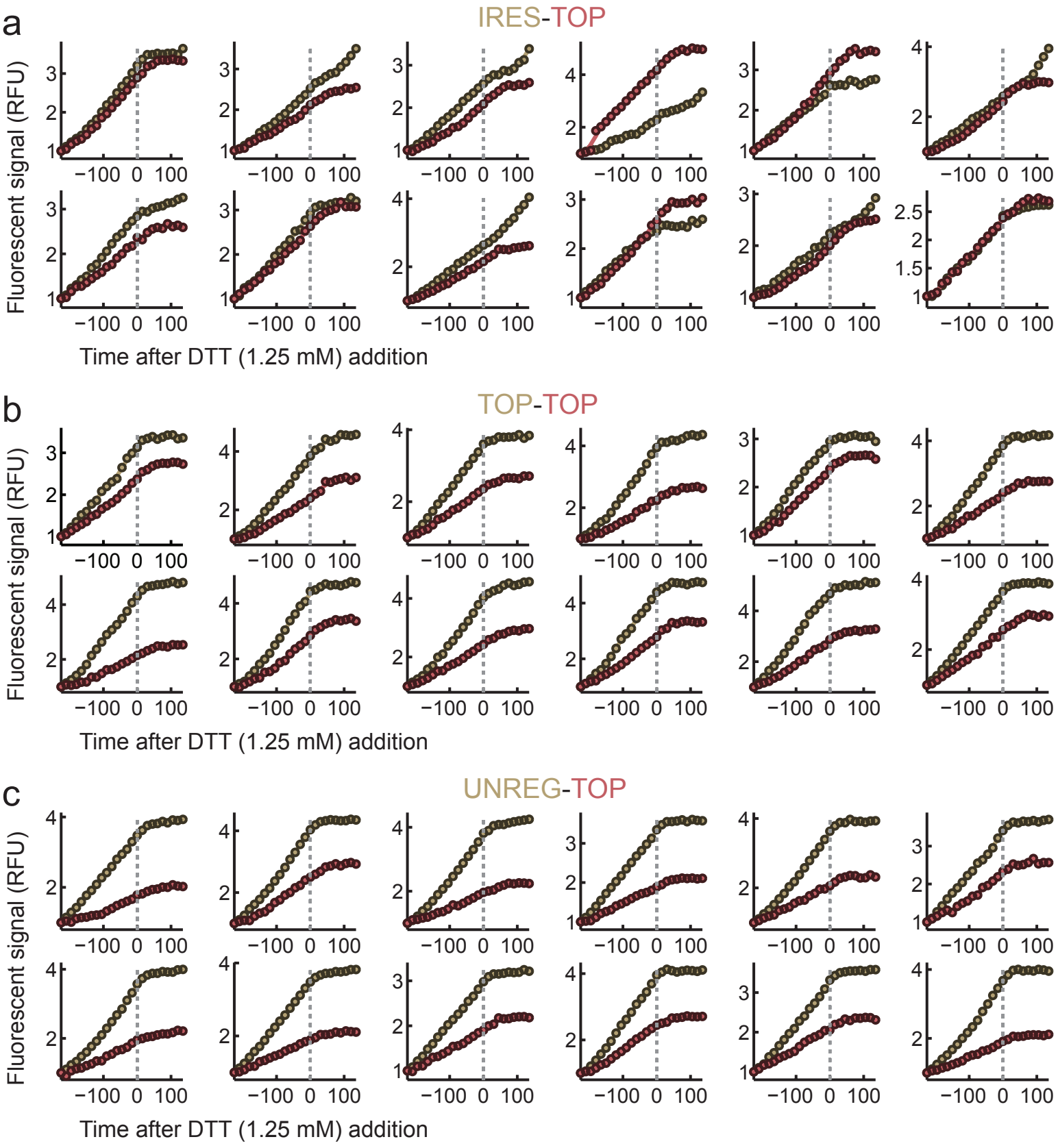

**Supplementary Figure 6: The IRES-reporter shows markedly different responses to DTT addition**

**(a)** The YFP (IRES) and mCherry (TOP) accumulation curves of the dual reporters from 12 representative single cells. DTT causes the decrease of YFP slopes in some of cells, whereas YFP slopes in the others are either unchanged or even slightly increased after DTT addition. Fluorescent intensity of each curve is normalized by its initial value. The mCherry slopes, on the other hand, show a uniform decrease. (**b**) The YFP (TOP) and mCherry (TOP) accumulation curves of the dual reporters from the 12 representative cells. (**c**) The YFP (UNST) and mCherry (TOP) accumulation curves of the dual reporters from the 12 representative cells.

# Supplementary Fig. 7

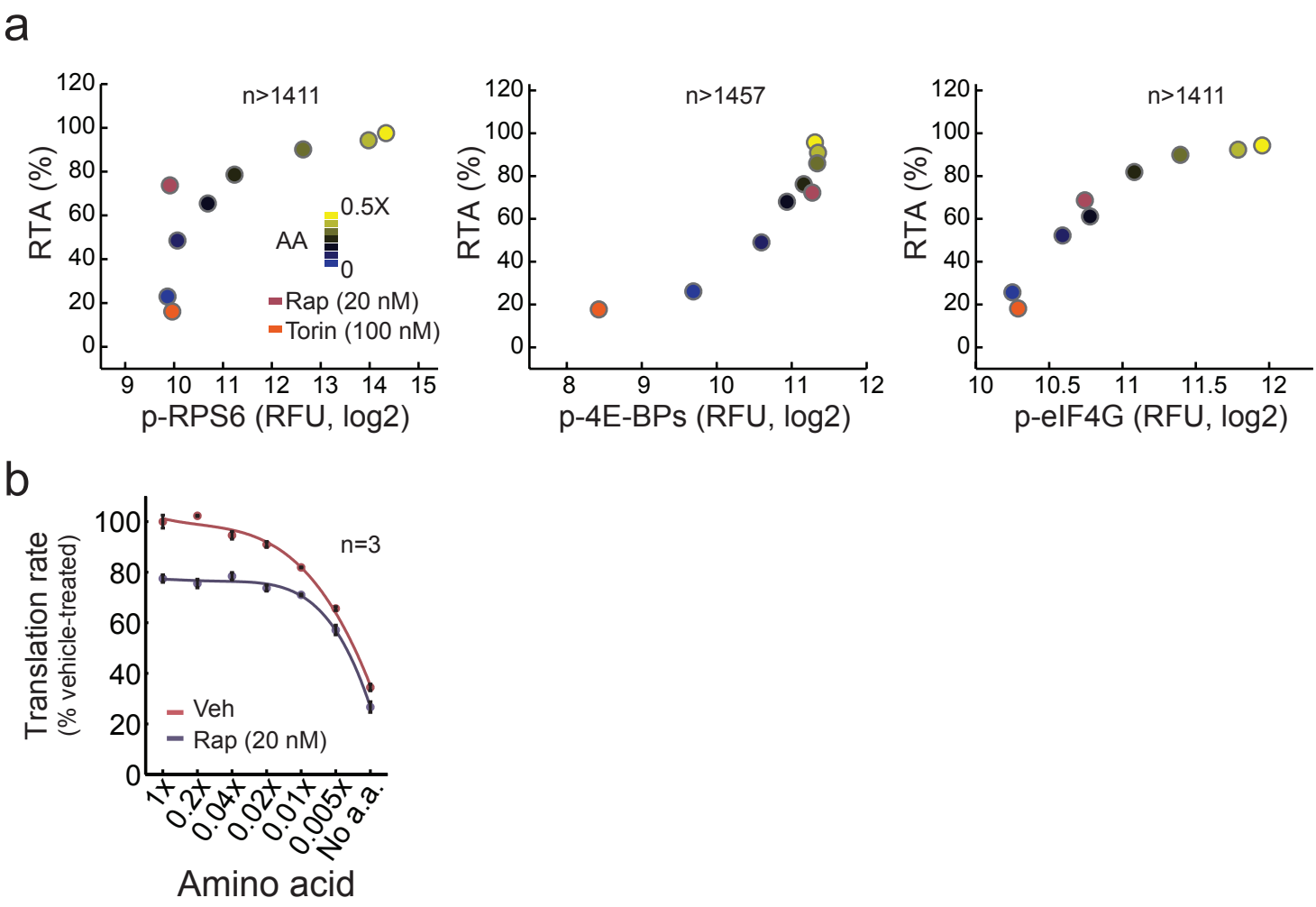


**Supplementary Figure 7: Correlation of phospho-RPS6, phospho-4E-BPs, and phospho-eIF4G with TOP translation upon amino-acid starvation and treatment with mTOR inhibitors.**

**(a)** The plotted correlation between phospho-eIF4G and RTA is similar to the correlation plots of phospho-RPS6. Rapamycin (20 nM) inhibits both phospho-RPS6 and phospho-eIF4G whereas phospho-4E-BPs is not affected. Amino acid concentrations mapped to the color bar: 0.5 (x), 0.1, 0.02, 0.01, 0.005, 0.0025, 0. **(b)** Mild amino-acid deprivation (from 1x down to 0.01x) cannot further decrease the RTAs of cells treated with rapamycin. Data from two wells of a 96-well plate are used to calculate the mean translation rate. Error bar shows s.e.m.

Nature Methods: doi:10.1038/nmeth.2729

# Supplementary Fig. 8

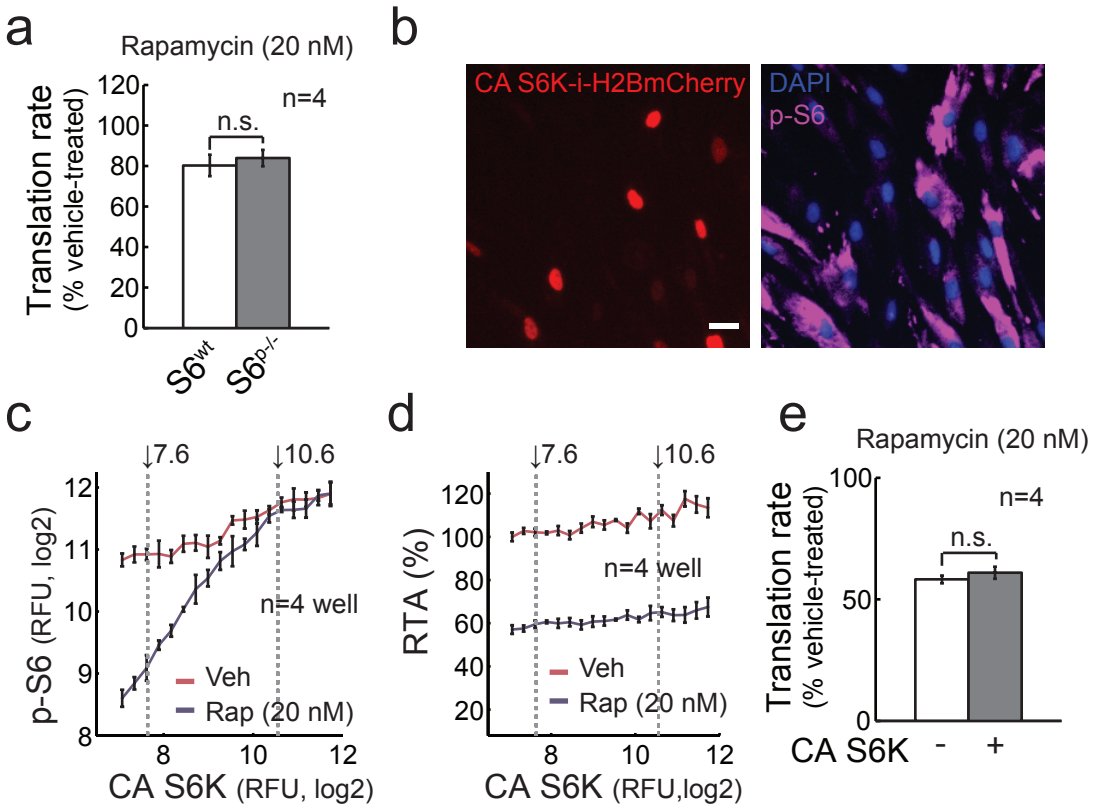


Nature Methods: doi:10.1038/nmeth.2729

**Supplementary Figure 8: A non-phosphorytable RPS6 mutant and constitutively active S6K (CA S6K) cannot rescue translational inhibition of TOP mRNAs by rapamycin.**

**(a)** RTA of WT MEFs and RPS6$^{p-/-}$ knock-in MEFs upon rapamycin treatment. The TOP reporters are stably transduced into the wild type and RPS6 $^{p-/-}$ knock-in MEFs, and RTAs are measured in both lines upon rapamycin treatment (20 nM). RTAs are again normalized by the RTAs acquired from the vehicle treated group on each cell line. Data from four wells of a 96-well plate are used to calculate the mean RTA. Error bar shows s.e.m. **(b)** Bj-5ta cells expressing CA S6K (red) have unaltered phospho-RPS6 levels (purple) even after rapamycin treatment. The amount of CA S6K per cell is estimated by the level of H2B-mCherry expressed by IRES on the same construct. **(c)** Joint distributions of CA S6K expression and phosphorylation of RPS6. CA S6Ks with IRES-driven mCherry marker are stably transduced into Bj-5ta cells expressing the TOP-YFP-reporter. Cells are binned by their mCherry levels and the mean of phospho-RPS6 intensities in each bin is measured in the control sample (Veh: red line) and the rapamycin treated sample (Rap: blue line). Error bars show s.e.m. **(d)** Joint distributions of CA S6K expression and translation (RTA) of the TOP reporter. RTA is measured in each bin as in **c**. Error bar shows s.e.m. **(e)** RTA of cells with and without CA S6K upon rapamycin treatment. Cells with mCherry levels less than 7.6 (RFU, log2) are considered as the CA S6K negative sample whereas cells with mCherry levels more than 10.6 are considered as the CA S6K positive sample. RTAs are measured on the both samples treated with rapamycin, and normalized by the RTAs acquired from

# Supplementary Fig. 9

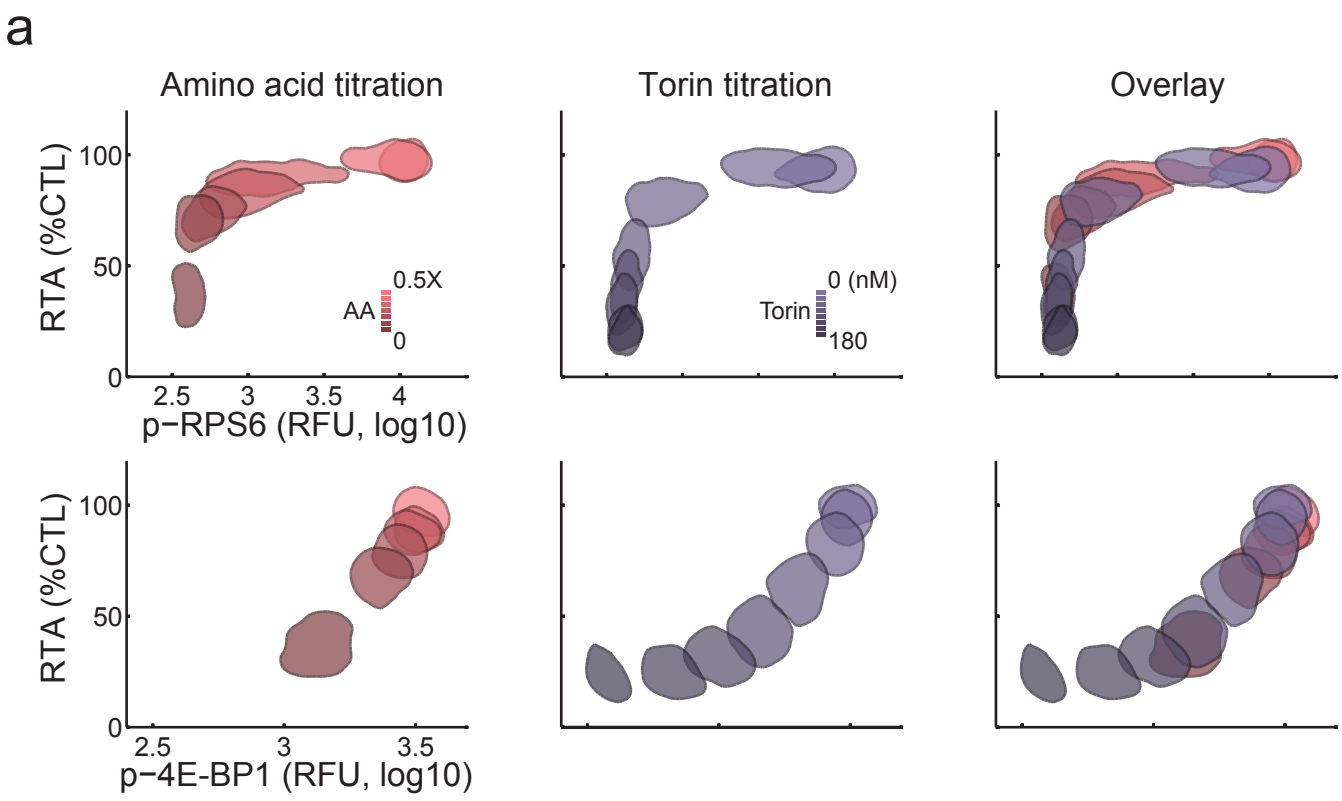


**Supplementary Figure 9: Amino acid starvation and direct mTOR inhibition generate similar patterns in the correlation plots.**

**(a)** The correlation contour plots between RTA and phosphorylations of mTORC1-targets in response to amino acid titration (left panel) and Torin2 titration (middle panel). The contour line is drawn in such a way that the data inside the contour represents the 25 % of the total cells. Amino acid concentrations mapped to the color bar: 0.5 (x), 0.1, 0.02, 0.01, 0.005, 0.0025, 0. Torin2 concentrations mapped to the color bar: 0 (nM), 1.5, 4.5, 13.5, 27, 40, 60, 90, 180. Phospho-RPS6 and phospho-4E-BPs intensities are plotted on a log10 scale.

# Supplementary Fig. 10

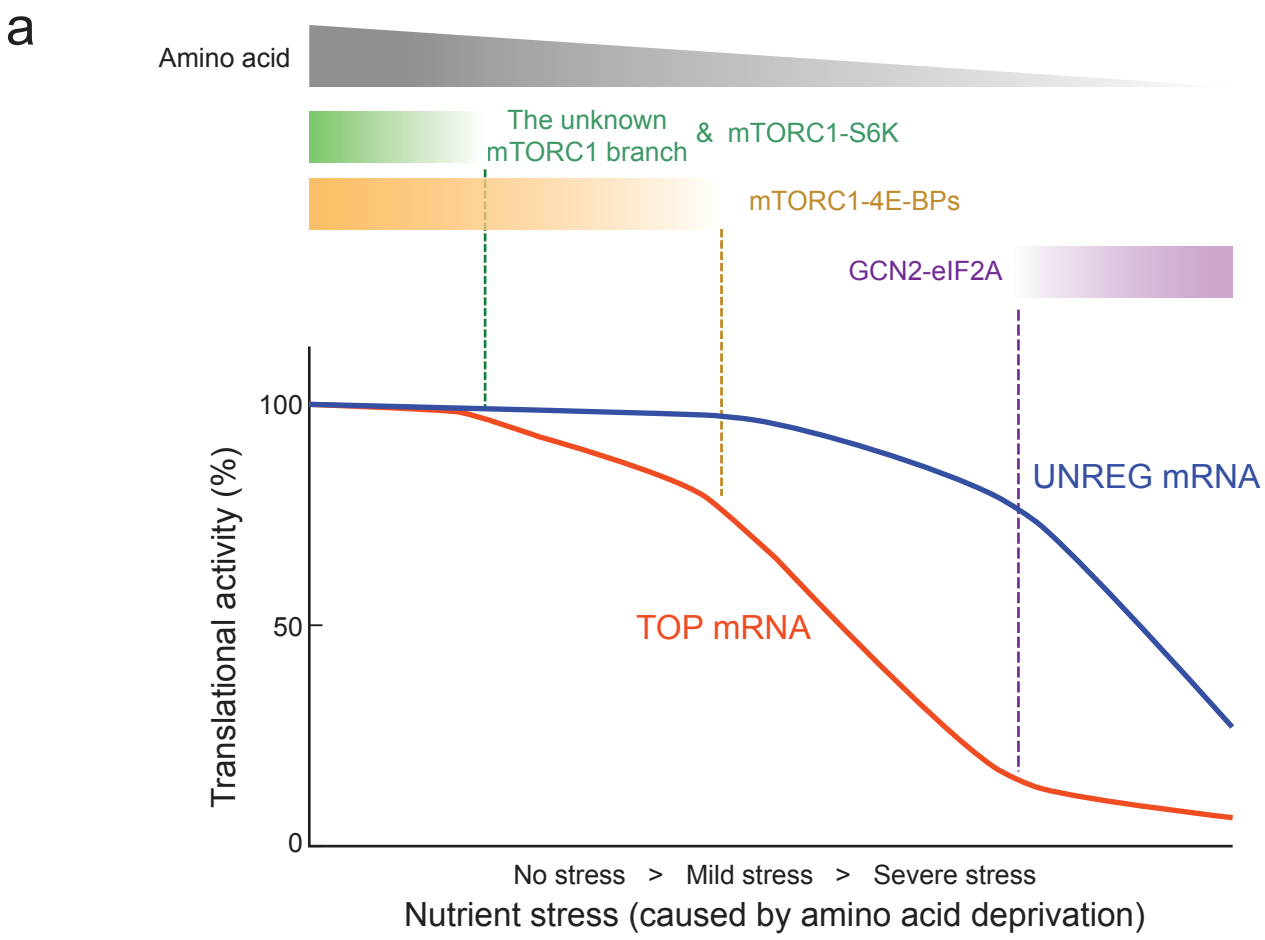


**Supplementary Figure 10: The proposed model for the control of TOP and UNREG mRNA translation during amino-acid limitation**

**(a)** The unknown, rapamycin-sensitive mTORC1 branch fine-tunes TOP mRNA translation during the mild reduction of amino-acid, whereas mTORC1-4E-BPs axis completely turns off translation of TOP mRNA when amino-acid levels largely drop. This would slow down the rate of amino-acid consumption, partly recover the balance between amino-acid supply and demand, and maintain the sufficient level of charged tRNA required for translation of UNREG mRNAs. However, when amino-acid levels further drop, GCN2-eIF2A pathway is activated to almost non-selectively decrease translation of both TOP and UNREG mRNAs.

# Supplementary Fig. 11

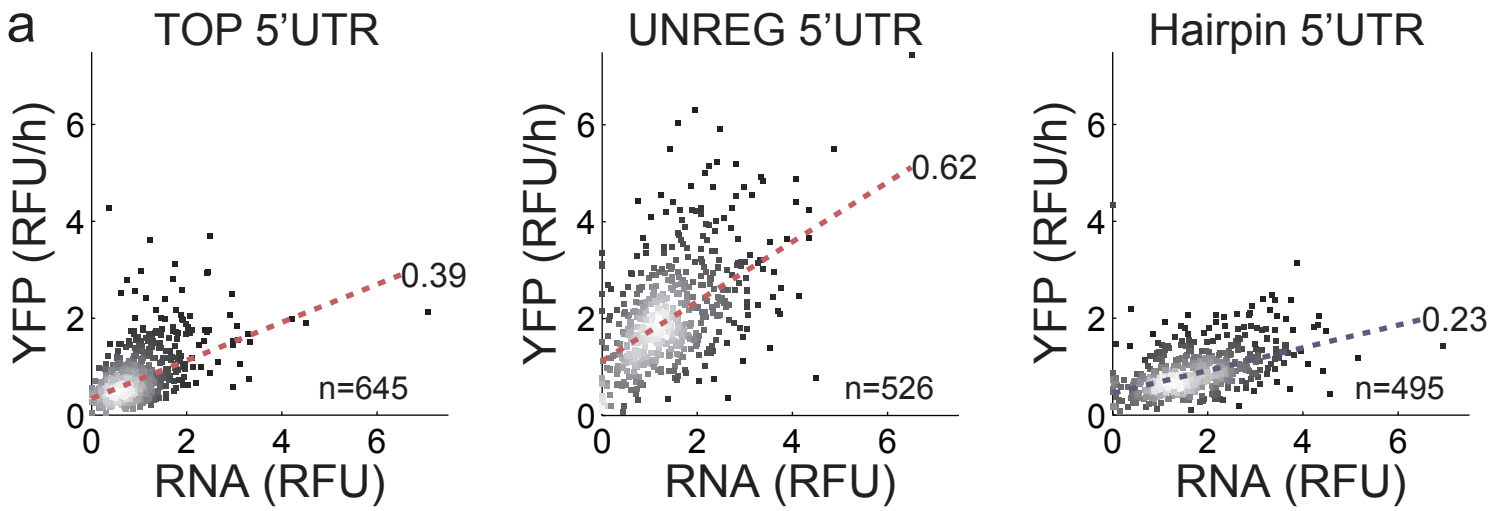


**Supplementary Figure 11: Measurement of the intrinsic effect of regulatory motifs on translation rate**

**(a)** The correlation plots between YFP accumulation rate (RFU / hour) and mRNA level (RFU) at the single-cell level. YFP slopes are first measured using a live-cell imaging protocol and the same cells are fixed and stained with a RNA FISH probe against the DHFR sequence to quantify mRNA levels on each cell. Three different reporters (TOP, UNREG, and Hairpin) are compared and their intrinsic effects on translation rates are estimated by the linear regression on the correlation plots. Hairpin construct has a hairpin (free energy estimated: -46 kcal/mol) in its 5'UTR.